Application Note

A Novel Series of Selective Agonists Evaluated against *Rattus Norvegicus* EP_4 Receptor

Melissa C. Holt[1], Rana Sidhu[1], Bill Ho[1], Fred L. Ciske[1], James B. Kramer[1], Joseph M. Colombo[1], Bradlee D. Germain[1], Andrei Kornilov[1], Adam Uzieblo[1], James P. O'Malley[2], Thomas A. Owen[2], Adam J. Stein[1], Ines M. Morano[1], and Stephen D. Barrett[1]

[1]Cayman Chemical and [2]Myometrics LLC

Key Features

- Cayman scientists deliver KMN-159, a novel, selective EP_4 receptor agonist with lower entropic costs of binding and increased affinity than other known agonists.
- KMN-159 was identified from a series of stereoisomerically pure EP_4 receptor-selective agonists evaluated by docking onto a rat EP_4 receptor model using AutoDock and Schrödinger.
- Continued development of novel, selective EP_4 agonists will further elucidate the role of this receptor and aid in the identification of novel therapeutics for bone growth, cardiovascular function, and disease.

Cayman Chemical · 1180 East Ellsworth Road · Ann Arbor, MI, 48108 · (800) 364-9897

Introduction

Prostaglandin E_2 (PGE_2) in humans is an almost ubiquitous arachidonic acid-COX cascade product that mainly mediates its multitude of signaling roles through activation of the GPCR superfamily-member E-type prostanoid receptors 1-4 ($EP_{1\text{-}4}$). The roles of functionally related EP_4 and EP_2 receptors have been widely investigated, and the receptors have been considered as therapeutic targets for a variety of indications including cancer, asthma, inflammation, heart failure, colitis, ischemia, and osteoporosis. Selective EP_4 and EP_2 modulators have been sought to provide the benefits of target modulation while limiting side effects arising from the modulation of the other receptor subtypes. Both EP_4 and EP_2 are coupled to G protein-dependent pathways through Gαs and, thus, activate adenylate cyclase and induce synthesis of intracellular cAMP.[1] Though EP_4 and EP_2 share overlapping functional roles, where they both are expressed in bone with roles in bone metabolism, they have only 38% homology in humans and are not pharmacologically identical.[2] Therefore, it is reasonable to target compounds that are highly selective for EP_4 receptors as therapeutic agents.[3,4]

Roche reported a potent γ-lactam EP_4 receptor agonist, Compound 31, referred to here as CAY10684 (Item No. 15966).[5] This compound displayed essentially no binding affinity for EP_2. The reported SAR suggested that replacing the PGE_2 ω-chain pentyl terminus with an aromatic ring exploited some difference between the EP_4 and EP_2 binding sites, leading to the observed selectivity. Docking studies illustrate the fit and key binding interactions of CAY10684 within EP_4 and EP_2 binding site amino acid residues. Using a structural biology approach, we describe herein a SAR series focused on ω-chain substitutions, utilizing an alkyne to provide rigidity. Additionally, the identification of the beneficial bis-fluorination of the γ-lactam greatly improved affinity. This work led to KMN-159, a novel, potent, and soluble EP_4-selective agonist. Furthermore, we suggest its likely binding mechanism through docking studies which align well with the SAR series, focusing on the benefits of the bis-fluorination on the improved docking of KMN-159 over KMN-80 (Item No. 15435).

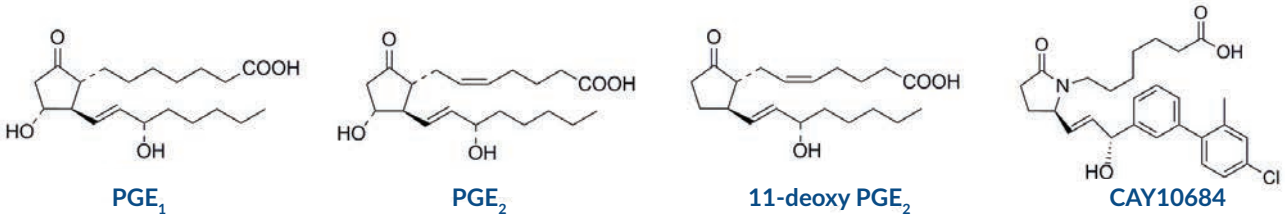

PGE_1 **PGE_2** **11-deoxy PGE_2** **CAY10684**

Figure 1. Select EP_4 receptor agonists

Methods

Rat EP_4 Receptor Reporter Assay

A batch of frozen HEK293T cells were prepared and stored in vapor phase of a liquid nitrogen vessel. Aliquot(s) of frozen HEK293T/17 cells were thawed and seeded onto a T150 tissue culture flask to allow recovery for 20-24 hours. Cells were harvested from the flasks and re-seeded on an EP_4 reporter assay plate (Item No. 600350) at a density of 65,000-75,000 cells/well in 200 µl reduced serum medium containing 0.5% FBS. Cells were incubated at 37°C with 5% CO_2 for 16-18 hours to allow expression of the receptor target. Culture media was aspirated and replenished with 100 µl serum-free culture medium. Test compounds were prepared at 2x final concentration and added to wells. For each compound, a 12-point dose-response curve (DRC) in 4-fold serial dilution was performed in triplicate. PGE_2 DRCs were run in parallel in all experiments (concentrations from 0-10 nM). After 6 hours of stimulation, 10 µl of media was transferred to a corresponding well of a 96-well solid white plate. The plate was heated at 65°C for 30 minutes to inactivate endogenous alkaline phosphatase. Luminescence-based alkaline phosphatase substrate (Item No. 600183) was added to each well and Secreted Embryonic Alkaline Phosphatase (SEAP) activity was measured by reading the luminescence signal after a 10 minute incubation. The EC_{50} values for PGE_2 and each test compound were calculated using GraphPad Prism 6 (GraphPad Prism version 6.00 for Windows, GraphPad Software, La Jolla California USA, www.graphpad.com). The methodology was performed with appropriate substitutions for assaying against rat EP_2 receptor.

Rat EP_4 Receptor and Rat EP_2 Receptor Homology Modeling[6]

The sequences for R. *norvegicus* EP_2 receptor and R. norvegicus EP_4 receptor were submitted to RaptorX structure prediction suite (http://raptorx.uchicago.edu/) and analyzed to confirm the quality of the model using the P-value, global distance test, absolute global quality, and RMSD. All metrics indicated the models were acceptable. RaptorX utilized squid and human rhodopsin as the primary templates for rat EP_4 threading and squid rhodopsin and rat neurotensin receptor 1 as the primary templates for rat EP_2 threading. For rEP_4, residues 1-16, 201-288, and 352-488 were identified as potentially disordered. For rEP_2, residues 1-17, 52-64, 227-257, and 324-357 were identified as potentially disordered. For both models, these regions largely consist of loops. The receptors were prepared for docking in AutoDock with MGLTools 1.5.7.

Rigid and Flexible Docking in AutoDock Vina[7]

Ligand 3D PDB files were generated utilizing CACTUS SMILES translator (http://cactus.nci.nih.gov), and the ligands were prepared with MGLTools 1.5.7. Rotatable bonds were introduced, amide bonds were held as fixed, and hydrogens were added. A search grid of 27,000 $Å^3$ centered on residue TYR188 with maximum exhaustiveness was used to dock ligands in rigid mode utilizing AutoDock Vina and the AMBER forcefield. Residues lining the various regions of the rigid binding-site were selected and prepared as flexible residues using MGLTools 1.5.7. Rotatable bonds were introduced, amide bonds were held as fixed, and hydrogens were added. Flexible residues in rEP_4 receptor were PHE28, PHE102, ASN164, SER185, TYR188, SER193, SER288, and ASP314. The same search grid as the rigid docking was used to search with maximum exhaustiveness to dock ligands in flexible mode utilizing AutoDock Vina. Ten poses per docking experiment were generated. Poses were evaluated by their score (kcal/mol), how often similar poses repeated, and consistency among multiple models. We sought out trends that were verified within multiple models and consistent with trends observed within cell-based data.

Induced Fit Docking with Schrödinger Maestro 11[8-13]

All files were prepared and generated within Maestro 11. Ligands were prepared with LIGPREP from SMILES using OPLS3 force field modified using EPIK. Molecules were desalted and featured all possible tautomers. Receptors were modified using Maestro Protein Preparation Wizard selecting default values. Positions of hydrogen bonds and torsion angles were refined prior to initiation. A search grid of 8,000 $Å^3$ was centered on residue TYR188 for rEP4 receptor docking. A search grid of 8,000 $Å^3$ was centered on residue SER121 for rEP_2 receptor docking. Glide docking was performed and subsequently refined with Prime to introduce residue flexibility within 5 Å of the binding site. Compounds were evaluated based on docking score, Emodel score, and GlideScore.

Results

The threading models generated by RaptorX for the rEP_4 receptor (**Figure 2B**) and rEP_2 receptor (**Figure 3A**) were validated within Maestro 11 and displayed strong metrics with P values of $4.6x10^{-7}$ and $1x10^{-6}$, respectively. The binding pockets for each receptor were identified with site map within Maestro 11. The size and shape of the individual receptor binding pockets were estimated to be highly distinct, with rEP_4R having a wide, deep pocket of 5,408 $Å^2$ (**Figure 2B**) and rEP_2R having a narrow, long pocket of 1,370 $Å^2$ (**Figure 3B**). The binding pose of PGE_2 within the rEP_4R is driven largely by hydrophobic interactions with the heptanoic acid α-chain, with key hydrophilic interactions being seen between the 11-hydroxyl, carboxylate, and 15-hydroxyl (**Figure 2B**). The 15-hydroxyl appears to be a hydrogen bond donor towards TYR188, with the 11-hydroxyl making a hydrogen bonding network with ANS324 and SER288. Within rEP_2R, the top PGE_2 pose displayed interactions between ASN307 and the 15-hydroxyl, hydrogen-dipole interactions between the carboxylate and SER87, and hydrogen bonding between ASP79 with the 11-hydroxyl (**Figure 3B**). The hydrophobic pocket within rEP_2R was smaller and likely the cause of the lower affinity of PGE_2 for rEP_2R relative to rEP_4R. Additionally, PGE_2 is seen to be much more conformationally restricted within the rEP_2R binding pocket, suggesting binding comes with higher entropic cost.

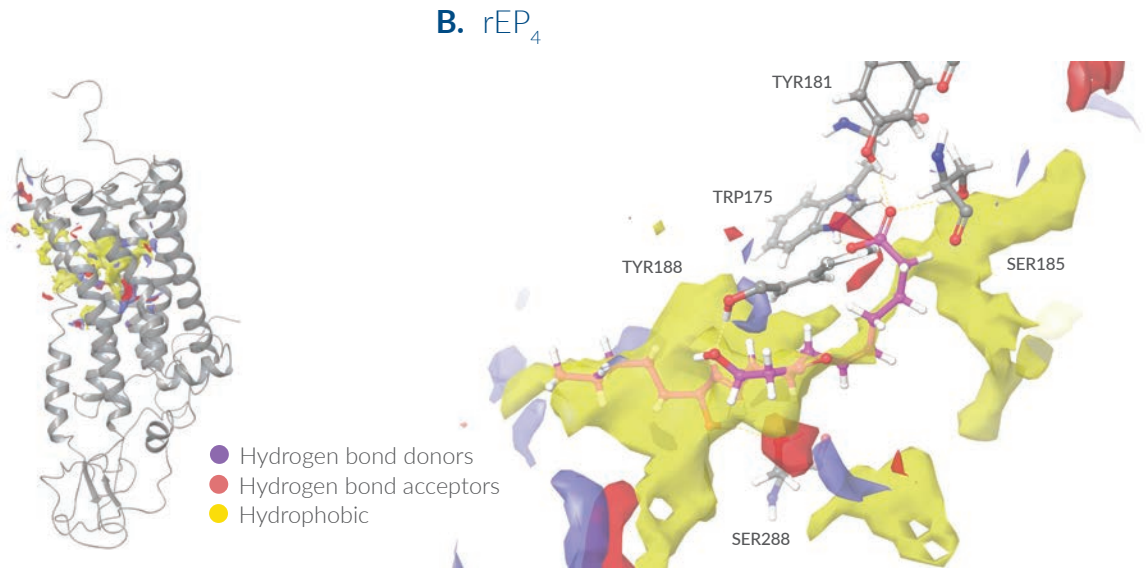

Figure 2. A. RaptorX model of rat EP_4 receptor with proposed ligand binding site identified and highlighted by Maestro 11 Ligand Site. **B.** Docking of PGE_2 into rEP_4 receptor model using a Maestro Induced Fit model, highlighting key interactions between the α-chain carboxylate with TYR181 and TRP175, 15-hydroxyl with SER288, and 11-hydroxyl with TYR188. Side chains are displayed in gray.

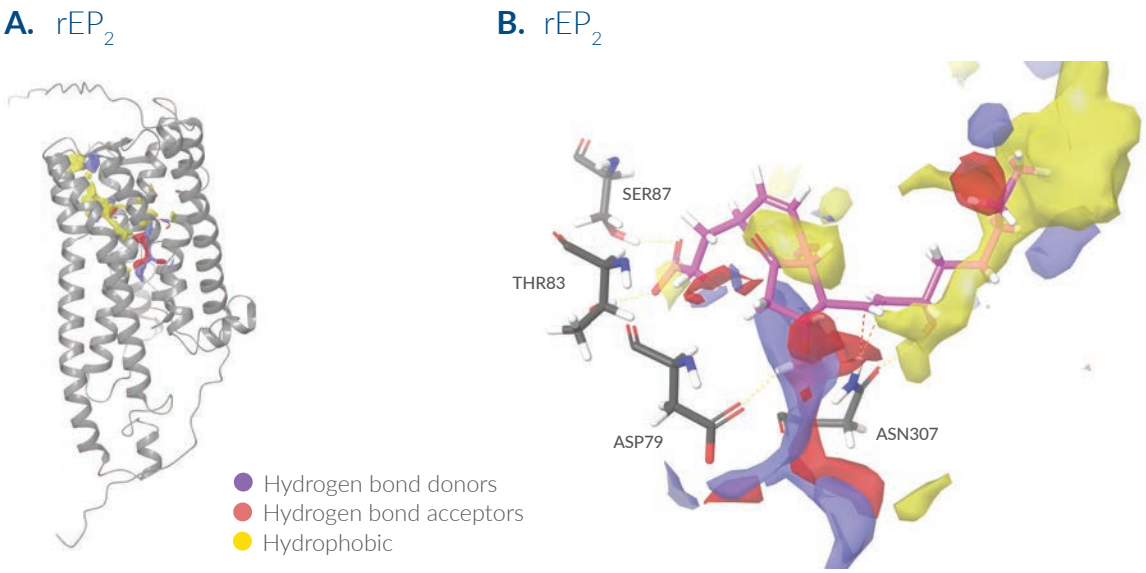

Figure 3. A. RaptorX model of rat EP_2 receptor with proposed ligand binding site identified and highlighted by Maestro 11 Ligand Site. **B.** Docking of PGE_2 into rEP_2 receptor model using a Maestro Induced Fit model, highlighting key interactions between the 11-hydroxyl with ASP79, α-chain carboxylate with SER87 and THR83, and 15-hydroxyl with ASN307. Side chains are displayed in gray.

Cayman has developed a series of novel agonists that utilize the heptanoic acid α-chain of PGE_1 and unique alkyne ω-chain, which attempt to mimic the rigidity of the ω-chain utilized within the Roche compound, CAY10684 (Item No. 15966) (**Figure 4A**). Previous work using a CRE SEAP reporter assay was used to validate the compounds as agonists with high selectivity for rEP_4R *versus* rEP_2R (**Figure 4B**). KMN-80 was determined to have an EC_{50} of 166 pM and >10 µM for rEP4R and rEP_2R, respectively (**Table 1**). KMN-159 was determined to have an EC_{50} of 26.5 pM and 4.9 µM for rEP_4R and rEP_2R, respectively (**Table 1**). Through our docking studies, we have identified several mechanisms driving the increased affinity of KMN-159 for rEP_4R, where the *bis*-fluorination of the lactam ring was the only difference between the compounds. Additionally, the phenomenon was observed regardless of the α- and ω-chains throughout Cayman's SAR efforts.

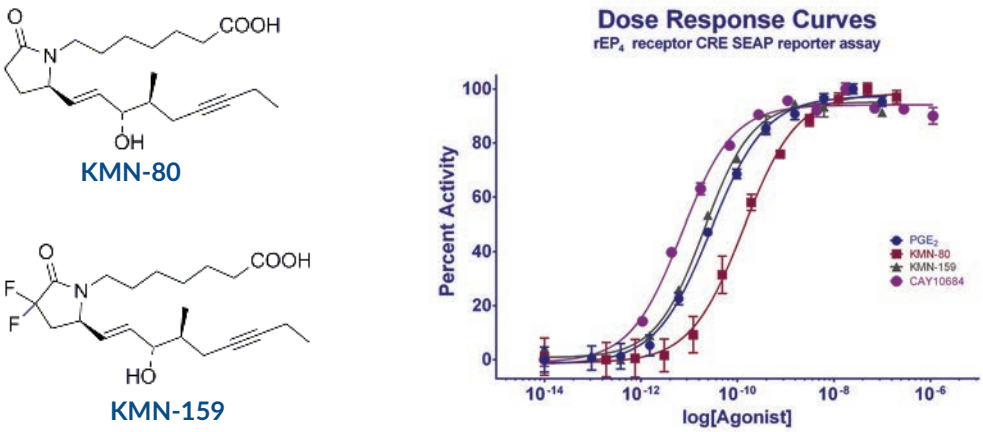

Figure 4. A. Structures of KMN-80 and KMN-159. **B.** Representative data from rEP_4 receptor CRE SEAP reporter assay displaying dose-response curves for PGE_2, KMN-80, KMN-159, and CAY10684.

Table 1 - Compiled data from rEP_4 receptor CRE SEAP reporter assay, rEP_2 receptor CRE SEAP reporter assay counter screen, AutoDock docking studies, and Schrödinger docking studies.

COMPOUND	EC_{50} (pM) rEP_4R	EC_{50} (nM) rEP_2R	RATIO EP_2/EP_4	rEP_4R AUTODOCK RIGID (kcal/mol)	rEP_2R AUTODOCK RIGID (kcal/mol)	rEP_4R AUTODOCK FLEXRES (kcal/mol)	rEP_4R MAESTRO INDUCED FIT (kcal/mol)	rEP_4R MAESTRO EMODEL	rEP_2R MAESTRO INDUCED FIT (kcal/mol)	rEP_2R MAESTRO EMODEL
PGE_1	21.3±3.6 (n=3)	4.4±0.4 (n=3)	206	-7.7	-6.9	-7.5	-10.72	-99.15	-11.08	-101.10
PGE_2	29.2±1.5 (n=56)	3.3 (n=16)	113	-7.9	-6.9	-8.5	-10.50	-99.20	-11.10	-113.72
11-deoxy PGE_2	36.9±10.7 (n=6)	38.71±4.48	1,049	-7.9	-7.3	-8.0	-9.77	-87.83	-10.58	-83.83
CAY10684	6.9±0.06 (n=3)	>5,000	>724,637	-8.9	-5.7	-9.7	-14.72	-149.97	-13.01	-116.56
KMN-159	26.5±2.7 (n=7)	4,900	184,905	-8.4	-6.3	-8.3	-11.81	-111.93	-11.21	-94.74
KMN-80	166.61±14 (n=6)	>10,000	>60,000	-7.7	-6.8	-7.9	-11.23	-103.06	-10.98	-94.47

The docking pose of PGE_2 served as the baseline pose for the docking study. A select series of compounds from Cayman's SAR series were docked against rEP_4R and rEP_2R, and the key differences resulting from the addition of the difluoro moiety were noted. The docking metrics for rEP_4R were much stronger, which is in line with the *in vitro* selectivity data, with lower docking scores, Emodel scores, and Einternal scores (**Table 1**). The Glide Emodel score *versus* the docking score displayed more linearity in the rEP_4R docking experiment, which is indicative of lower conformational costs associated with the poses (**Figure 5**). KMN-159 and KMN-80 displayed a pose that was very similar to PGE_2 within rEP_4R (**Figure 6A**). The docking scores for KMN-159 and KMN-80 were -11.81 kcal/mol and -11.23 kcal/mol, respectively and the Emodel scores, -112 and -103, respectively (**Table 1**). This matches with the rank order observed in the *in vitro* assay. The heptanoic acid α-chain was observed to have some flexibility, displaying varying poses in the computational experiment. KMN-80 was observed interacting with TYR181 and SER185 in the top pose. For KMN-159, this was observed to be TRP174 and SER185 in the top pose. Likely, compounds that included more bulk would be able to occupy a larger portion of this hydrophobic pocket but would require polarity at the terminus to exploit the hydrophilic regions at the bottom of the pocket. SER193 was observed to interact with the lactam carbonyl in each compound. The 15-hydroxyl, which is considered the key interaction for the agonist pharmacophore, was observed to make an interaction with ASN324 in KMN-159 but not KMN-80 (**Figure 6A** *versus* **Figure 6B**). It was also observed that KMN-159 displayed a nearly flat ring in the top pose *versus* KMN-80, which displayed a puckered ring (**Figure 8**). This would be expected by the inclusion of the fluorines, which due to their smaller anti-bonding orbitals relative to hydrogen, have an increased tendency to be gauche to the carbonyl oxygen.[14] As the lactam ring features an SP_2 nitrogen, the increased flatness of the ring results in lower internal strain within the ring. The conformational locking of the ring results in lower entropic costs with binding as well. Using surface representations of the binding surface and compound surface for KMN-159 and KMN-80, we observed that KMN-159 filled the binding pocket to a larger extent, partially due to its altered position where it is shifted by 2Å and partly due to the slightly larger Van der Waals radius of the difluoro (**Figure 7**). These features, along with the addition of the beneficial hydrogen bond with the 15-hydroxyl within KMN-159, are thought to be the contributing forces behind the 5x higher affinity of KMN-159 *versus* KMN-80.

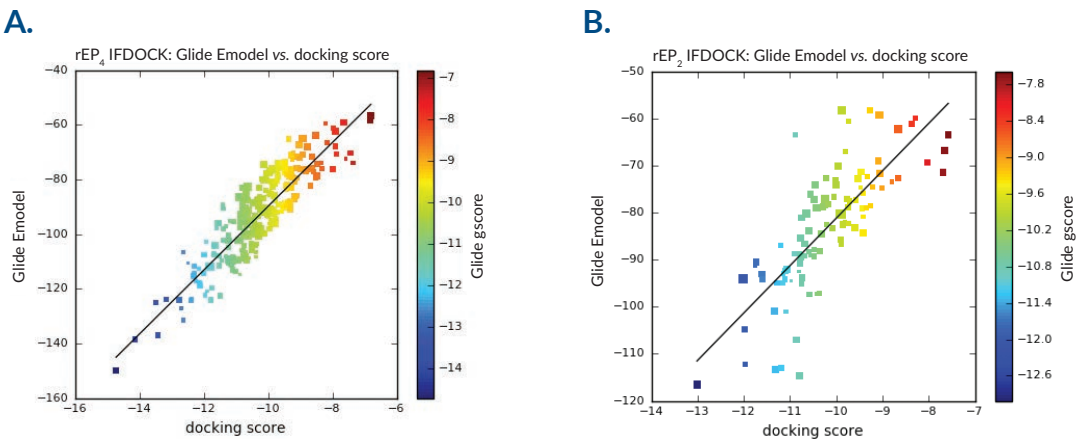

Figure 5. Plot of docking score (kcal/mol) versus emodel score for compounds docked against rEP_4 receptor. **B.** Emodel score versus docking score for ligands docked against rEP_2. Poses with higher internal strain display higher Emodel scores and are ranked lower than poses with low Emodel scores (more negative). All data points are colored based on Glide gscore, a metric similar to docking score. The points are sized according to their Glide Einternal score, a measure of torsional strain, where smaller indicates less strain.

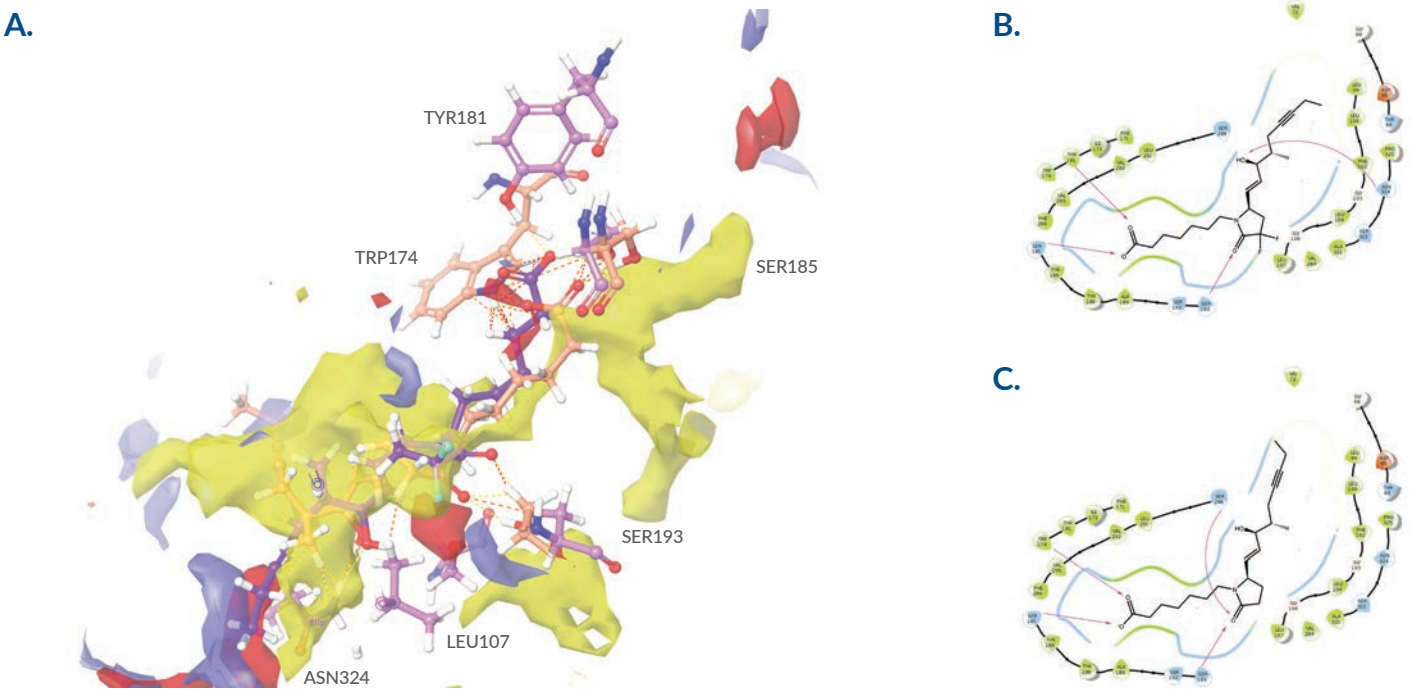

Figure 6. A. Compound overlay of KMN-159 and KMN-80 to rEP_4 receptor generated from Maestro 11 Induced Fit model featuring site map. Side chains for each flexible dock are shown in either pale purple or pale orange. **B.** Key interactions for KMN-159 in 2D plot. **C.** Key interactions for KMN-80 in 2D plot.

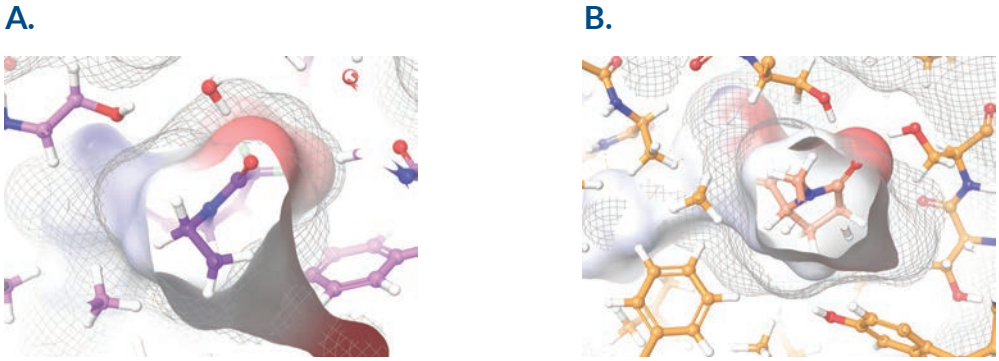

Figure 7. A. Top docking pose of KMN-159 rEP_4 receptor generated from Maestro 11 Induced Fit model featuring surface representation of receptor and ligand binding site. **B.** Top docking pose of KMN-80 rEP_4 receptor generated from Maestro 11 Induced Fit model featuring surface representation of receptor and ligand binding site.

A. **B.**

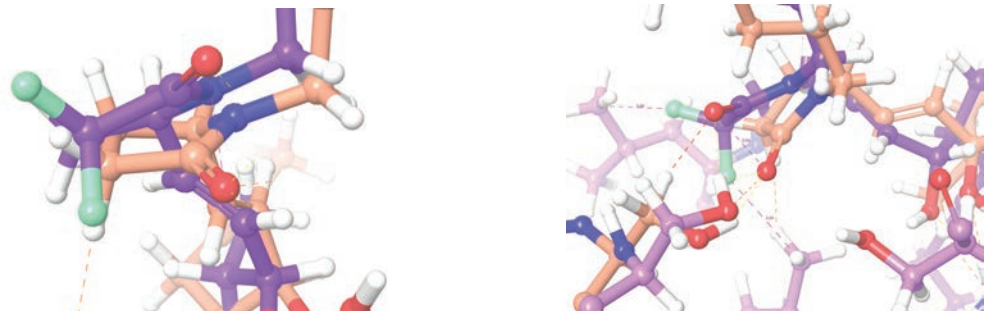

Figure 8. A. Zoom in of puckered KMN-80 ring. **B.** Zoom in of flat KMN-159 ring.

Lastly, we highlighted how the Roche compound, CAY10684, displays the strongest docking metrics of any compound within this study (**Table 1**). The binding mode was exceptionally similar to KMN-159, where the main difference appeared to be that the increased bulk of the ω-chain exploited the binding pocket to a higher extent (**Figure 9**). Likewise, KMN-159 and CAY10684 displayed inferior docking metrics when docked against rEP_2R. KMN-159 sat at the top of the binding pocket and did not overlay well with PGE_2 (**Figure 10A**). CAY10684 sat at the bottom of the binding pocket and partially overlaid with PGE_2. The ω-chain did not overlay and appeared to be too bulky for the base of the binding pocket (**Figure 10B**). These studies helped to add rationale to the observed experimental data of the in vitro SAR work.

A. rEP_4 **B.**

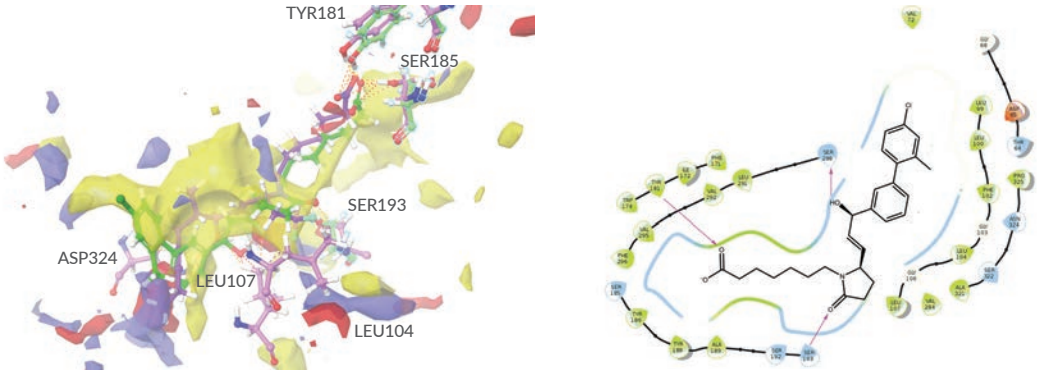

Figure 9. A. Compound overlay of KMN-159 and CAY10684 featuring site map. Side chains for each flexible dock are shown in either pale purple or pale green. **B.** Key interactions of CAY10684 in 2D plot.

A. rEP_2 **B.** rEP_2

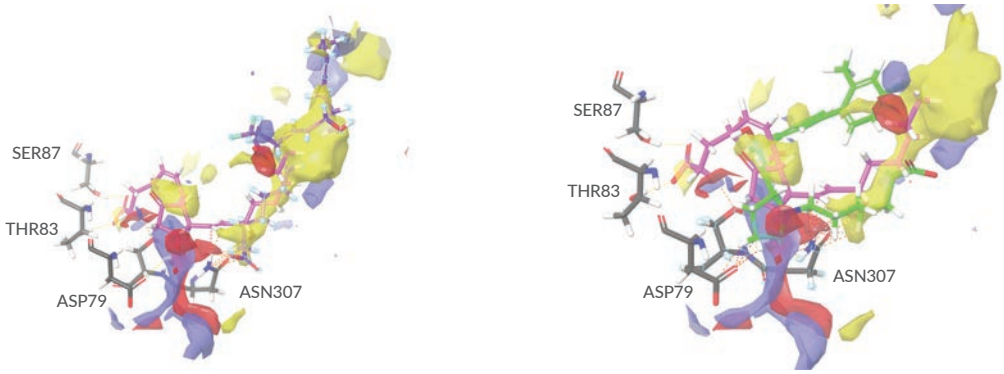

Figure 10. A. Binding mode of PGE_2 with overlay of KMN-159 in rEP_2 Maestro 11 Induced Fit model featuring site map. Note that KMN-159 does not sit in bottom of pocket like PGE_2. Side chains forming PGE_2 binding pocket are ASP79, THR83, SER87, and ASN307 (gray). ASN307 makes a polar contact with KMN-159 carboxylate. **B.** Binding mode of PGE_2 with overlay of CAY10684 in rEP_2 Maestro 11 Induced Fit model featuring site map. Note that CAY10684 does not overlap well and displays high internal torsion metrics.

Conclusions

Key interactions were highlighted from this docking study regarding the binding of a series of novel rEP$_4$ receptor agonists. The lactam carbonyl is seen interacting with SER193 in nearly all compounds. A large hydrophobic pocket has been identified, which likely could be further exploited in the KMN series. SER185 is seen commonly locking the α-chain carboxylate into place. Additionally, TYR181 and TRP174 are seen interacting with the α-chain carboxylate in some cases and not others. The 15-hydroxyl displayed the greatest variability and sensitivity in its interactions. In the case of KMN-80 *versus* KMN-159, we postulate that the increased size of the difluoro, coupled with the conformationally locked, flat nature of the 159 γ-lactam, shifts the docked position of KMN-159 to create a more favorable hydrogen bonding interaction with the 15-hydroxyl relative to KMN-80 at a lower entropic cost. The increased potency of KMN-159 is a result of the interaction of the 15-hydroxyl with ASN324 and coordination of LEU104 and LEU107 by the difluoro moiety. These beneficial interactions are not present in KMN-80. KMN-159 displayed a very similar binding mode relative to CAY10684. CAY10684 displayed very strong metrics within the binding experiment. Additionally, compounds docked against the rEP$_2$ receptor displayed poorer metrics and did not overlay well with the natural substrates, particularly PGE$_2$. These docking studies have allowed the interpretation of the SAR work in greater detail. The addition of the difluoro moiety is thought to play a small steric role, shifting the position of the lactam ring slightly, conformationally locking the γ-lactam, and improving the coordination of the carboxylate and 15-hydroxyl with their
associated binding niches.

Cayman products used in this application

EP$_4$ Agonists

Item No.	Product Name
15966	CAY10684
13010	Prostaglandin E$_1$
14010	Prostaglandin E$_2$
14520	11-deoxy Prostaglandin E$_2$
15435	KMN-80
Custom	KMN-159

Assay and Kit Components

Item No.	Product Name
600340	EP$_2$ Receptor (rat) Reporter Assay Kit
600350	EP$_4$ Receptor (rat) Reporter Assay Kit
600183	SEAP Substrate (Luminescence)

References

1. Sugimoto, Y. and Narumiya, S. *J. Biol. Chem.* **282(16)**, 11613-11617 (2007).
2. Blackwell, K.A., Raisz, L.G., and Pilbeam, C.C. *Trends Endocrinol. Metab.* **21(5)**, 294-301 (2010).
3. Ke, H.Z., Crawford, D.T., Qi, H., *et al. J. Bone Miner. Res.* **21(4)**, 565-575 (2006).
4. Weinrab, M., Grosskopf, A., and Shir, N. Am. *J. Physiol. Endocrinol. Metab.* **276(2)**, E376-E383 (1999)
5. Elworthy, T.R., Kertesz, D.J., Kim, W., *et al. Bioorg. Med. Chem. Lett.* **14(7)**, 1655-1659 (2004).
6. Källberg, M., Wang, H., Wang, S., *et al. Nat. Protoc.* **7(8)**, 1511-1522 (2012).
7. Seeliger, D. and de Groot, B.L. *J. Comput. Aided Mol. Des.* **24(5)**, 417-422 (2010).
8. Friesner, R.A., Murphy, R.B., Repasky, M.P., *et al. J. Med. Chem.* **49(21)**, 6177-6196 (2006).
9. Halgren, T.A., Murphy, R.B., Friesner, R.A., *et al. J. Med. Chem.* **47(7)**, 1750-1759 (2004).
10. Friesner, R.A., Banks, J.L., Murphy, R.B., *et al. J. Med. Chem.* **47(7)**, 1739-1749 (2004).
11. Farid, R., Day, T., Friesner, R.A., *et al. Bioorg. Med. Chem.* **14(9)**, 3160-3173 (2006).
12. Sherman, W., Day, T., Jacobson, M.P., *et al. J. Med. Chem.* **49(2)**, 534-553 (2006).
13. Sherman, W., Beard, H.S., and Farid, R. Chem. *Biol. Drug Des.* **67(1)**, 83-84 (2006).
14. Gillis, E.P., Eastman, K.J., Hill, M.D., *et al.* Applications of fluorine in medicinal chemistry. *J. Med. Chem.* **58(21)**, 8315-8359 (2015).

Cayman Chemical · 1180 East Ellsworth Road · Ann Arbor, MI, 48108 · (800) 364-9897